Basrah Journal for Engineering Sciences, Vol. 24, No. 1, (2024), 109-119

Review Article

Journal homepage: www.bjes.edu.iq
ISSN (Online): 23118385, ISSN (Print): 18146120

A Review of Intelligent Techniques Based Speed Control of Brushless DC Motor (BLDC)

Husam Jawad Ali [1, *], Diyah Kammel Shary [2], Hayder Dawood Abbood [3]

[1,2,3] *Department of Electrical Power Techniques Engineering, Southern Technical University, Basrah, Iraq*
E-mail addresses: hussam.jawad@fgs.stu.edu.iq , diyahpower@stu.edu.iq , habbood@stu.edu.iq
Received: 1 November 2023; Revised: 20 January 2024; Accepted: 1 February 2024; Published: 15 February 2024

Abstract

This study uses intelligent techniques to regulate brushless direct current speed (BLDC) motors. After these motors solved the problem of using brushes and commutators in traditional DC motors, they succeeded in replacing brushes and commutators with electronic commutators. Due to the use of electronic switching, brushless motor algorithms are more complex than those of conventional motors. In this study, to adjust the PID controller's settings (Kp, Ki, and Kd), a trial-and-error approach was taken, and a completely new method known as the settings of known PID controllers have been modified using the new Gray Wolf algorithm. A BLDC motor's main benefit is that it has easy speed adjustment across a broad range, whereas AC motors often cannot be controlled in this way. Through the use of Matlab/Simulink, the BLDC motor's mathematical model was developed and implemented. The simulation results show that in the first case, a PID controller effectively induces the turbulent dynamic behavior of BLDC under load and no-load conditions, and in the second case, the speed shows the lowest rise time, stability, overshoot, and stability conditions, and performs at its best. The characteristics of the traditional PID controller that regulates the engine speed must be regulated online to achieve the use of intelligent technologies, and the adjustment is done online using the neural network. The results showed that this technology, or feature - online tuning - is the most effective and reliable of all.

Keywords: BLDC motor, PID controller, GWO, Speed control, Neural network.

https://doi.org/10.33971/bjes.24.1.12

1. Introduction

The brushless direct-current motor (BLDCM) is a synchronous motor with permanent magnets on the rotor and stator winding. In the future, it must develop motor controllers for engineering applications through simple and economical design. The BLDCM can be expanded to an operation speed range more than the base speed using Artificial Intelligence Technique (AI). It is necessary to use a controller that can improve the performance of the three-phase BLDC motor. The speed response of the BLDCM system with control units PID can be tuned effectively by optimizing the parameters of the PID controller using artificial intelligence algorithms. in recent years, DC motors have become increasingly popular due to their advantages such as extensive speed control and high efficiency. However, commutators and brushes might be considered a significant drawback of such motors due to the ongoing deterioration of these parts, which ultimately increases safety risks and maintenance costs. However, Brushless BLDC motors have provided a solution to this problem. Several studies have been conducted on optimizing BLDC motor design using electric circuits instead of commutators and brushes [1, 3]. In comparison to induction motors and brushed DC motors, BLDC motors have a number of benefits. The stability of the drive will be aided by features like a long service life, quiet operation, high efficiency, high dynamic response, wide speed range, low temperature, and the capacity to withstand shock and vibration [4, 5]. The control algorithm for this motor is more complex than that for other types of engines since it uses electronic commutation. In order to obtain a comprehensive and exquisite control strategy for the BLDC motor, an accurate model is necessary. As a result, the motor model serves as the brain of the control drive [6]. An example of a synchronous motor is a (BLDC) motor, which has permanent magnets on the rotor and stator winding. It is commonly utilized in instruments, hard drives, robotics, cars, and aircraft [7]. Single-phase, two-phase, and three-phase BLDC motors are the three different varieties. Three-phase motors are the most common and widely used. In terms of torque-current characteristics and torque-speed characteristics, BLDC motors are similar to DC motors. The rotor moves or rotates due to a moving magnetic field, similar to AC motors [8]. A permanent synchronous motor with rotor position feedback is known as a BLDC motor. Typically, a three-phase power semiconductor bridge is used to drive it. Instead of employing brushes to commutate the BLDC motor, its three-phase inverter uses the position of the rotor as feedback. The rotor's position is necessary for the motor to start and to provide the correct sequence of commutation to regulate the power devices in the inverter bridge. The motor comprises a stator winding fed by rectangular stator currents and has a permanent magnet rotor that generates trapezoidal back-EMF waves and, theoretically, constant torque. The BLDC motor's operation is established by the inverter's phase switching when it turns two phases ON simultaneously while the rest phase floats. The two phases are successively energized and changed every 60 degrees depending on the rotor position [6, 9]. The (Inrunner) and (Outrunner) are the two main categories of BLDC motors. The two types' structures are depicted in Figs. 1 (a) and (b). Inside the fixed component of the in-runner

motor are permanent magnets. This type is superior to the (Outrunner) type in situations where high speed is required. Applications requiring low torque and high speed typically utilize this kind. Although they spin less slowly, (Outrunner) motors provide more torque. This kind is a quitter for applications requiring strong torque and low speed [8, 10, 11].

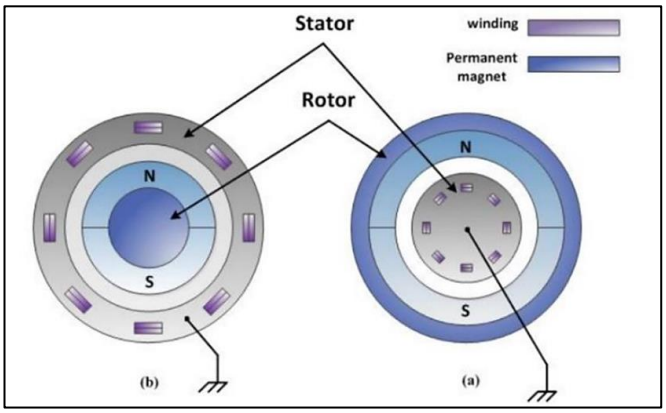

Fig. 1 BLDC motor types, (a) In-runner, (b) Out-runner [10], [11].

Stators in BLDC motors have axially cut slots along the inner perimeter of the stacked steel laminations. The stator windings of the motor of a BLDC are arranged in a star or delta pattern. Stators are linked in a star arrangement in the majority of BLDC motors. These windings are made up of many coupled coils. Forming a winding involves putting a coil in a slot and connecting it to another coil as shown in Fig. 2 [10]. Stator windings can be divided into two types: trapezoidal and sinusoidal motors. This differentiation is established to provide the diverse forms of back electromotive forces. It is based on the stator windings; coils are interconnected (EMF). A trapezoidal motor's back EMF is generated in a trapezoidal manner, and that of a sinusoidal motor is sinusoidal, as their names suggest. The matching kinds show sinusoidal and trapezoidal variations in the phase current, as does the motor's back EMF. For this reason, the torque output of a sinusoidal motor is smoother than that of a trapezoidal motor. But this comes at an extra expense since sinusoidal motors need more winding connections because of the way the coils are distributed around the perimeter of the stator, which increases the amount of copper that enters the stator windings. having the ability to choose a motor depending on the control power supply capacity that has the proper stator voltage rating. Robotics, small arm motion, and other fields use motors rated for 48 volts or less in their operations. Motors rated at 60–100 volts or above are used in industrial applications, automation, and appliances [12].

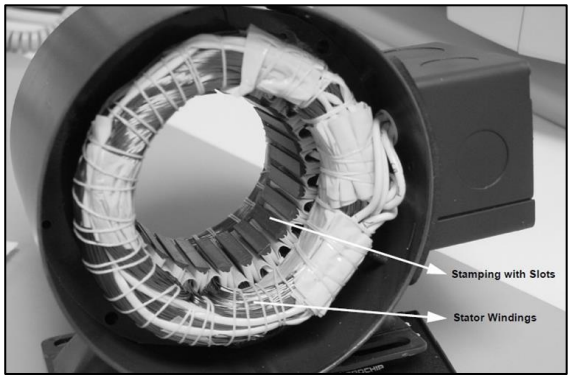

Fig. 2 Stator structure of a BLDC motor [10].

Magnet materials and pole pairs make up the rotor. The right magnetic material to utilize to achieve the necessary magnetic field density in the rotor is determined by that need. Permanent magnets are often created using ferrite magnets. Due to their high magnetic density magnets made of rare earth alloys are large in becoming more and more common. Although ferrite magnets are less costly than alloys, one disadvantage is that they have a low flux density for the volume in question. On the other hand, rare earth alloy materials boost the motor's size-to-weight ratio and output a lot of torque for a motor of a comparable size. Some rare earth magnet alloys that have gained popularity recently include neodymium, ferrite, and boron (NdFeB). In order to compress the rotor even further, research is being done to increase the flux density. Figure 3 displays the cross-sections of many magnet configurations inside a rotor. There are various cross-sections for the rotor magnet [8], [12], [13]:

1. Magnets are positioned around a circular core.
2. Rectangular-shaped magnets are attached to a circular core embedded in the rotor.
3. Rectangular magnets attached to a circular core are inserted into the rotor core.

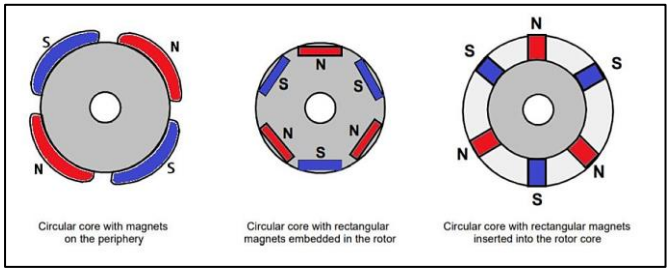

Fig. 3 Magnet rotor cross sections [14].

One of the crucial elements to increase a product's viability is system efficiency. Due to improvements in materials and design, the Brushless DC Motor's cost has decreased since it was first introduced. DC motor that is brushless is a popular part in many different applications due to its lower price as well as the several benefits it offers above the DC Brush Motor. Utilized is the brushless DC motor for a variety of purposes, including but not restricted to [11], [15]:

1. Instruments, and appliances equipment medical.
2. Transportation.
3. Equipment for Factory Automation.
4. Military.
5. Aerospace.

Lenz's Law states that every coil in a BLDC motor generates a voltage known as the reverse electromotive force, or back emf, which is in opposition to the coil's primary voltage. This voltage is known as the trapezoidal shape of the back phase EMF in a PMBLDC motor and its relationship to speed (Wm) and rotor position angle (θe). The construction of (bemfs) depends on three different factors, the rotor's angular speed, the magnetic field it generates, and the stator windings' number of turns. In BLDC motors, the rear emf has a trapezoidal form, unlike the sinusoidal shape of the back emf in PMSM. Different background EMFs are produced by BLDC motors and PMSMs depending on the physical conditions, the logic behind how the stator windings is coupled, and the winding. The differences between a BLDC motor and a PMSM are displayed in Table 1. Every motor has

a 3-phase balanced voltage with a 120-degree angle that separates each component from the back emf. Figures 4 and 5 show the back emf in PMSM and BLDC motors, respectively [8], [16].

Table 1. compares the differences between PMSM and BLDC motors.

No.	Feature	PMSM	BLDC
1	Back emf	Sinusoidal back emf	Trapezoidal back emf
2	Flux density (in space)	Sinusoidal distributions	Square distribution
3	Stator current	Sinusoidal wave	Square wave
4	Total power	Constant	Constant
5	Electromagnetic torque	Constant	Constant
6	Energized phases	Three phases are on at any time	Two phases are on at any time

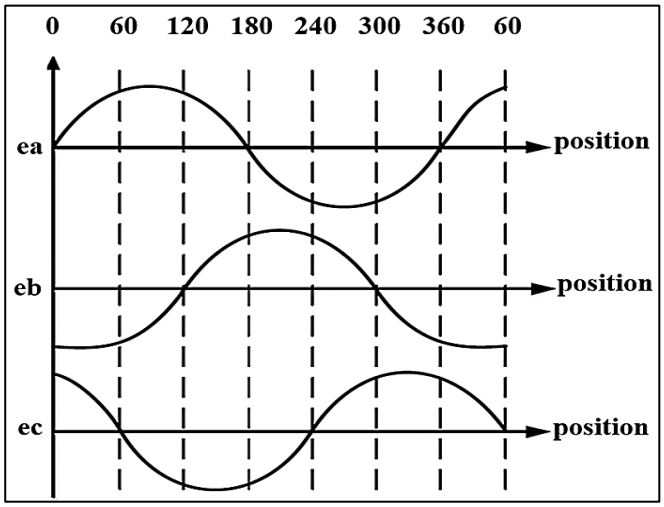

Fig. 4 Back-emf of PMSM motor [17].

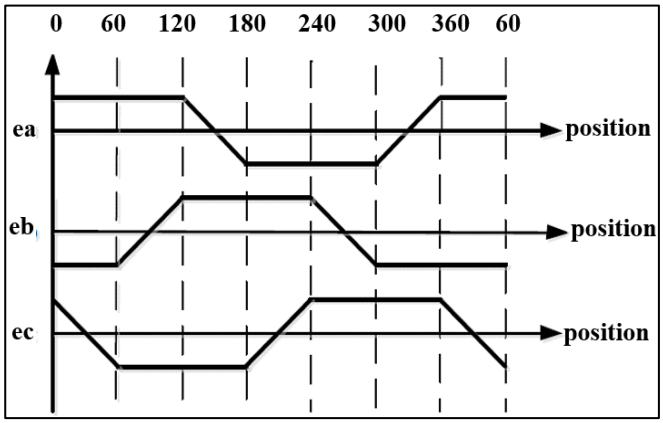

Fig. 5 Back-emf BLDC motor [17], [18].

All of these systems are mechanical and electrical because of their rapid dynamics and instability, they share the characteristic of feedback to the variable to be manipulated, usually position or speed, in order to change the command signal. However, a three-phase inverter with rotor position feedback must energize the stator coil of the BLDC motor in order to turn it on. In order for the motor to start and provide the correct switching sequences to operate a rotor position sensor is needed for the bridge inverter's power device. To choose which coils to activate, it's critical to comprehend the rotor's position. The position of the rotor is determined using a variety of techniques. In order to implement these strategies, the following strategies must be used [8], [12].

1. Hall sensor technology.
2. Background electromotive force detection technology.
3. Speed estimation technique.

In this research, the background EMF detection technology uses a Sensorless control method. Traditional PID control with simple closed-loop speed control methods is the control technique that control applications employ the most frequently, and if the parameters are recreated correctly, it can work stably with the majority of electronics. However, the biggest drawback of a PID controller is how difficult it is to implement gains in a perfect loop. This unit controls the system, its energy, and its dynamic regime [8], [19]. The technique used in this paper is described below.

For back EMF trapezoidal synchronous permanent magnet motors, proper phase current is essential. Any phase errors in the switching signals result in signals that cannot provide pulsating torque and increased copper loss in the BLDC motor. In this paper, back-emf and zero-cross point detection circuits are used for rotor position estimation and provide approaches utilizing zero-sensor detection of BLDC motor line voltages. With the proposed methods, the three-phase line voltage of a BLDC motor must be measured independently [20]. EMF detection technology at the back causes the third coil of the BLDC motor to float, leaving only two phases operating at any given moment. The electromagnetic field at the back is reduced using a floating coil, and a concept detection system is presented. The float coil terminal voltage is monitored to ensure that the back emf exceeds zero with respect to the neutral point voltage. Back EMF voltage is the name given to the neutral point of the motor. By comparing the terminal voltage to the neutral point, the neutral back emf can be determined. The neutral point of the engine is often unavailable. The most common approach is to create a virtual neutral point, which will theoretically have the same Y-turn capability as the engine, and then look for any differences [12], [21].

2. Operation principle of brushless DC motor

A brushless DC motor, which is classified as a permanent synchronous machine with rotor position feedback, operates through a three-phase bridge inverter that drives the motor in sync with the rotor position. To achieve proper operation and initiate the motor, a rotor position sensor is required. Additionally, this sensor is responsible for delivering the accurate commutation sequence, which subsequently activates the power devices in the inverter bridge. The commutation of these power devices occurs progressively every 60 degrees, contingent upon the rotor position. It's crucial to remember that this motor falls under the category of electronic motors, as it utilizes electronic commutation to switch the armature current instead of relying on traditional brushes. This design choice significantly enhances the durability of the brushless DC motor when compared to its DC motor counterpart, as it effectively eliminates common issues associated with the brush and commutator arrangement, such as sparking and brush wear-out. The implementation of the ideal speed control regarding the brushless DC a motor may observed in Fig. 6, showcasing the practical application of this advanced motor technology [16], [22].

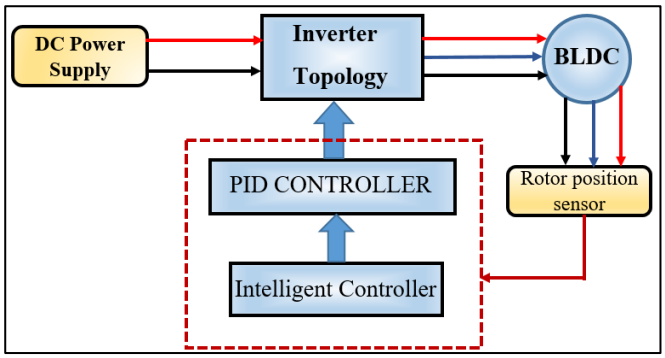

Fig. 6 Implementation of optimized speed control for BLDC motor.

The basic block diagram of a brushless DC motor is shown in Fig. 7. The four main parts of a brushless DC motor are the power inverter, sensors, control algorithms, and permanent magnet synchronous machine (BLDC).

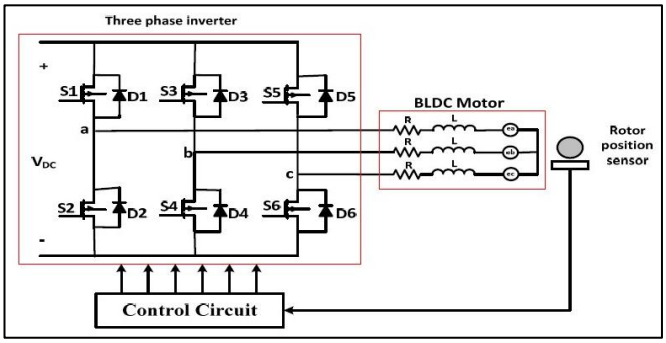

Fig. 7 three-phase inverter of BLDC motor drive [23].

Power is transferred from the source to the BLDC motor by the power inverter, which then translates electrical energy into mechanical energy. One of the best advantages of the brushless DC motor is the sensors for rotor position. The control algorithms choose the gate signals for each semiconductor in the power electronic inverter based on the rotor position and command signals, which might be torque, voltage, speed, or other instructions [16].

The BLDC motor runs in a two-phase-ON mode, during each commutation sequence, as illustrated in Fig. 3, the first winding is energized with positive power, signifying that the current enters the winding. In contrast, the second winding is energized with negative power, indicating that the current departs the winding. Simultaneously, the third winding remains floating, as exemplified in the diagram. The interplay between the magnetic fields generated by the stator coils and the magnetic field within the rotor magnet serves as a signal to each semiconductor within the power electronic inverter as shown in Fig. 8. This signal ultimately gives rise to the torque when the two phases are energized [24].

The main stage of power conversion is the inverter bridge, and the direction, speed, and torque that the motor produces are controlled by the switching patterns of the power devices. Bipolar or, more frequently, power MOS devices can be used as power switches. It is also feasible to use systems with mixed device inverters, such as those that use MOSFETs for the low-side switches and p-n-p Darlington's for the high-side power switches. The switching frequency of an inverter can range from 3 kHz to 20 kHz and higher [25].

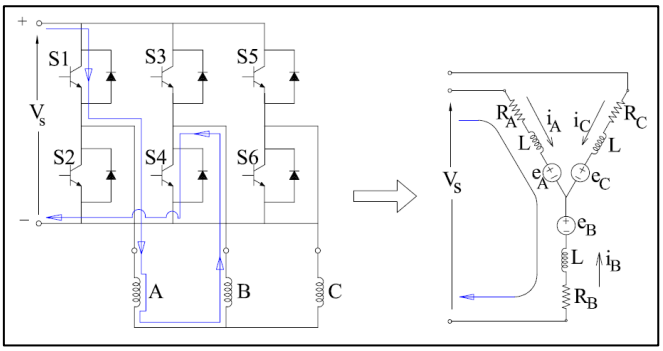

Fig. 8 The inverter circuit where phase A to phase B the currents flow [26].

3. Conventional PID control

The need to increase productivity imposes new requirements on mechanisms related to electric drives in most industrial processes, such as those in the development sites, paper, petroleum, electrical, mechanical, iron and steel, and construction industries. They cause a variety of operational challenges due to their unstable and rapid dynamics. The most crucial step in utilizing a PID controller is parameter setup. Most of the engineering convenience nowadays is provided by self-tuning PID controllers. The value of PID controllers comes from their broad application to the majority of control systems. Even if they don't always offer the best control, PID control systems have been shown to be beneficial high-resolution systems [12], [27]. The usual form of the typical PID control law is:

$$u(t) = kp.e(t) + ki\int_0^t e(t).dt + kd\frac{de(t)}{dt} \quad (1)$$

As a proportional gain, Derived gain Kp, Kd is the integral income, and e(t) is the error in derivatives [28], [29]. Tuning PID Controller Parameters in the industrial community, PID controllers with simple structures and reliable performance are frequently used. In this case, the proportion (P) plus integration (I) plus derivation (D) must be set, to have an impact on the PID controller's performance. For example, the improvement of the transient response with the PD controller may occasionally be hampered by the decrease of the steady-state error with the PI controller, and vice versa. Over-designing the controller for the system's steady-state error or transient response will therefore lead the accounting system to additional costs or other design problems. The manual trial-and-error method has historically been used to optimize PID controllers, which makes the processing time and labor intensive [8]. Block representation of a conventional PID Fig. 9 depicts the controller.

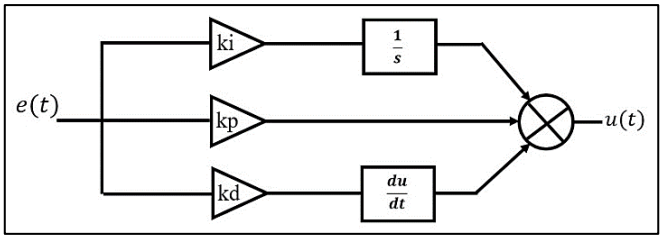

Fig. 9 Traditional PID controller.

The importance of optimization parameters or the outcomes of an operation used as input to the optimization algorithm are both described by the mathematical concept known as the objective function. The PID controller is used to decrease error signals and to choose a preferred alternative that will be applied with all optimization techniques to obtain a smaller error. Calculating the objective function yields:

$$ISE = \int e^2(t)dt \quad (2)$$

Where, ISE is the Integral square error fitness value, the control output, or time error signal, is denoted by u(t), and the error between the measured process output variable and a desired set point is represented by e(t).

4. Grey wolf optimization-based PID controller

In 2014, gray wolves were proposed by Mirjalili et al. using calculations representing social male gray wolves. The social hierarchy will appear, and the structure of this group will be determined by Fig. 10 [30], [31], [32].

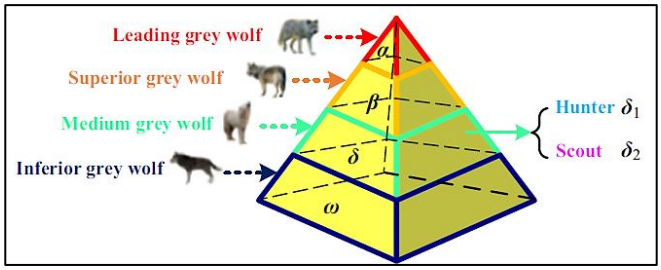

Fig. 10 Grey wolf hierarchy descending dominance [33].

This algorithm uses a hunting strategy to find and pursue prey (solution). There are three essential phases to hunting:

1. Tracking, pursuing, and approaching the target.
2. Circumnavigating the prey and moving it to stop it from moving.
3. pursuing the prey and taking it by force.

Four Groups, Beta, Delta, and Omega-are established in this algorithm, the gray wolves, are known to live in packs, the design phase seeks to reflect and replicate the complex social system observed within this species. With a hierarchical structure as an organizational framework, wolves serve as a great model for developing solutions. At the forefront of these solutions is Alpha, which represents the highest rank, while Beta and Delta occupy the next two positions in second and third places, respectively. However, the remaining substituents are considered relatively less important and are therefore classified under the term omega. This classification underscores the idea that these options have a decreasing degree of importance within the larger framework of the design phase [30], [34].

Figure 11 illustrate the method and style designed for hunting in addition, grey wolves' social hierarchy to model the style is the mathematical model that will represent GWO and its use in improving performance [35].

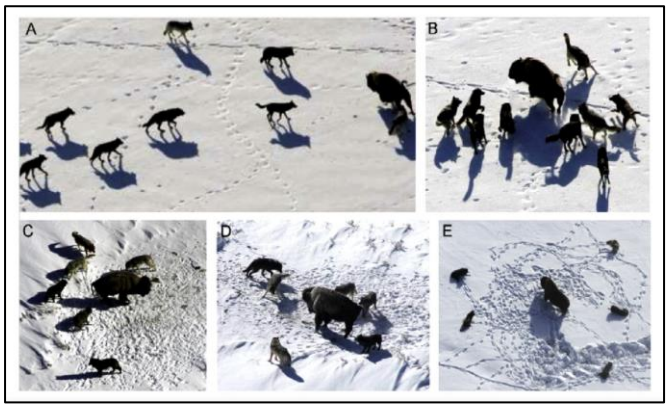

Fig. 11 Grey wolf hunting behavior is depicted in (A) approaching prey, (B) stalking, (C) harassment, (D) encirclement, and (E) attack state [30].

The prey tends to diverge from potential solutions when |A|>1 and move in defining the prey's direction when |A|<1 as shown in Fig. 12 [30].

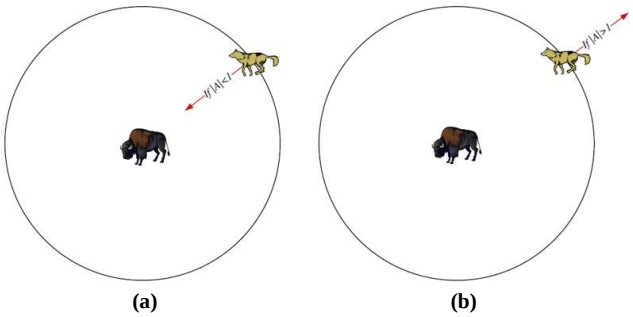

Fig. 12 (a) converge when |A|<1, **(b)** diverge when |A|>1.

Grey wolves circle their prey while hunting, as was already mentioned. To represent encircling behavior analytically, equations provided are as follows [36]:

$$\vec{D} = \left|\vec{C}\vec{X}_P(t) - \vec{X}(t)\right| \quad (3)$$

$$\vec{X}(t+1) = \vec{X}_P(t) - \vec{A}.\vec{D} \quad (4)$$

In addition, the iteration, prey position, and grey wolves are all indicated by the (t) symbol. Moreover, the coefficient vector can be computed in the manner described below [33], [37]:

$$\vec{X}_1, \vec{X}_2, \vec{X}_3 \quad (5)$$

$$\vec{C} = 2^* \vec{r}_2 \quad (6)$$

$$\vec{a} = 2 - 2\frac{t}{\max\_iter} \quad (7)$$

Where,

$\vec{D}$: A grey wolf's distance is defined by these terms.
$\vec{A}$, $\vec{C}$: Coefficient vectors are referred to by these terms.
r_1 and r_2 are randomly chosen between one and zero and their values range from A decrease of 2 to 0.

In this case, it is feasible to clarify neighbors in Fig. 13 using a two-dimensional location vector in order to understand the impacts of Eqns. (3) and (4). Grey wolves are in position (X, Y), as seen in Fig. 13 (a). Its location can be changed in accordance with the prey's position (X*, Y*). By changing the value and vectors, it is possible to attain the best agents for the given situation in a number of locations. When the 3D grey wolf spot is updated, as shown in Fig. 13 (b), grey wolves can alter their location inside the area surrounding their prey using Eqns. (3) and (4) [38], [39].

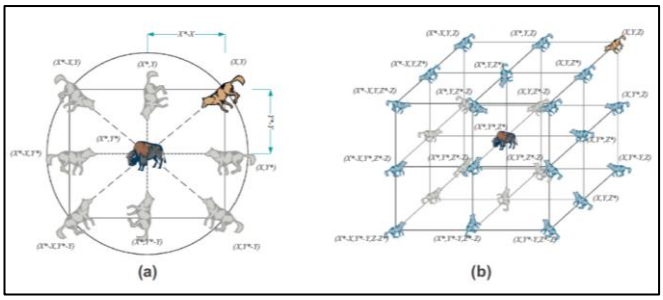

Fig. 13 Position vectors in 2D and 3D and their possible future locations [39].

Groups that hunt cooperatively, there will be three wolves leading the pack, and there are three wolves, which are called the leaders. who typically possess the most professional and practical expertise, as well as possibly the most trustworthy information on the precise location of (best) perspective in order to catch prey and engage in a well-organized hunt. As shown in Fig. 14.

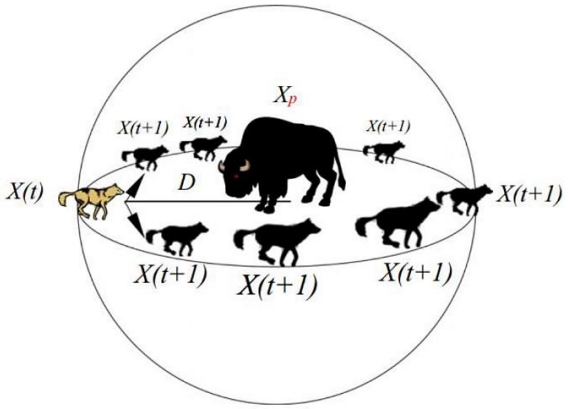

Fig. 14 Update on Wolf's position [31].

The wolves will then be led, they should update their positions based on the new information discovered locations of the leaders. Based on eq. (4) to (7), the updated laws of places are as follows [38]:

$$\begin{aligned} \overrightarrow{D}_\alpha &= \left|\overrightarrow{C}_1.\overrightarrow{X}_\alpha - \overrightarrow{X}\right| \\ \overrightarrow{D}_\beta &= \left|\overrightarrow{C}_2.\overrightarrow{X}_\beta - \overrightarrow{X}\right| \\ \overrightarrow{D}_\delta &= \left|\overrightarrow{C}_1.\overrightarrow{X}_\delta - \overrightarrow{X}\right| \end{aligned} \tag{8}$$

$$\begin{aligned} \overrightarrow{X}_1 &= \overrightarrow{X}_\alpha - \overrightarrow{A}_1.(\overrightarrow{D}_\alpha) \\ \overrightarrow{X}_2 &= \overrightarrow{X}_\beta - \overrightarrow{A}_2.(\overrightarrow{D}_\beta) \\ \overrightarrow{X}_3 &= \overrightarrow{X}_\delta - \overrightarrow{A}_3.(\overrightarrow{D}_\delta) \end{aligned} \tag{9}$$

$$\overrightarrow{X}(t+1) = \frac{\overrightarrow{X}_1 + \overrightarrow{X}_2 + \overrightarrow{X}_3}{3} \tag{10}$$

Where,

$\overrightarrow{A_1}$, $\overrightarrow{A_2}$, and $\overrightarrow{A_3}$ define the coefficient vectors and $\overrightarrow{C_1}$, $\overrightarrow{C_2}$, $\overrightarrow{C_3}$, Prey location and position $\overrightarrow{X_\alpha}, \overrightarrow{X_\beta}, \overrightarrow{X_\delta}$, Grey wolves' position $\vec{X}$, Grey wolves' distances $\overrightarrow{D_\alpha}, \overrightarrow{D_\beta}, \overrightarrow{D_\delta}$, Grey wolves and their positions $\overrightarrow{X_1}, \overrightarrow{X_2}, \overrightarrow{X_3}$.

A flowchart diagram of detection and updating using the parameters and equations indicated in Fig. 15 can be used to illustrate the GWO technique.

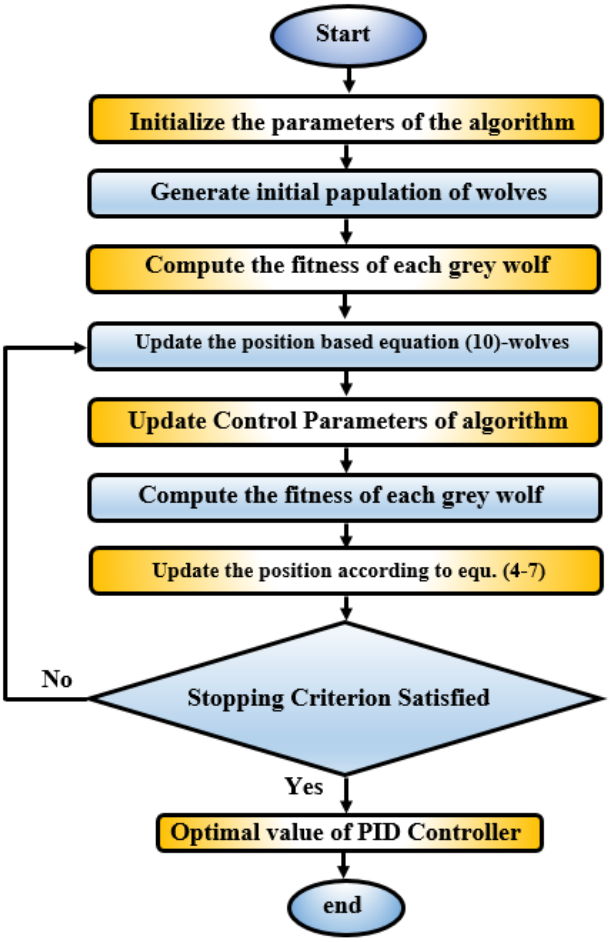

Fig. 15 Adaptive GWO algorithm flowchart [38].

5. Neural network-based PID controller design

A brushless motor, being an inherently non-linear system, presents a challenge in obtaining an optimal response of a BLDC motor using conventional linear control methods. As a result, conventional PID controllers are considered insufficient due to the nonlinear nature of the brushless motor model, necessitating the development of alternative control methods. This paper deals with the performance and accuracy requirements for implementing a BLDC motor position control system by combining a PID controller utilizing a neural

network created artificially, and a position control system for BLDC motors has been developed based on an internal backpropagation neural network, and the PID parameters are set accordingly. The present work presents a PID neural network architecture designed for a BLDC driver [40].

A comprehensive investigation will be conducted on the BLDC motor's performance under the suggested control scheme, taking into account various effects of changes in speed and torque. Furthermore, PID neural control is examined in-depth and compared with conventional PID and Gray Wolf Optimization techniques.

The motor control mechanism for the BLDC is an intricate, nonlinear, system with multiple variables that provide flexible and adaptable capabilities. The use of intelligent controllers for BLDC motors has gained significant interest in recent years. One such method is neural control, which utilizes Artificial Neural Networks (ANNs) to control the system based on the system's dynamic behavior. This approach is very appropriate for adaptive control systems where the control unit must adapt to changes in the system's behavior. In this study, ANN was employed to build a BLDC motor speed control inverse model [41].

The resulting inverse model was then utilized as a console to create the BLDC motor's speed control mechanism. The suggested controller can withstand disturbances and changes in the system's properties. The study also emphasizes how crucial it is to have a thorough model of the BLDC motor in order to create an effective control system. The control system that has been suggested possesses the capability to be utilized in a vast array of industrial sectors, thereby signifying its versatility and potential for widespread implementation, such as robotics, electric vehicles, and aerospace systems. The utilization of a visual depiction regarding the necessary elements to execute the project effectively confirms the veracity of the speed control pertaining by the application of an artificial neural network to the BLDC motor [43], which can be observed in Fig. 16, which comprises a MATLAB-designed Simulink block in the form of a schematic block diagram featuring multiple blocks.

When utilizing neural networks to facilitate online optimization of PID control parameters, the approach is highly efficacious. The neural network receives the error (e), which is the difference between the actual and intended locations, and the speed (N) of the BLDC motor as input. The neural network, in turn, generates outputs pertaining to proportional, integrative, and derivative gain modification.

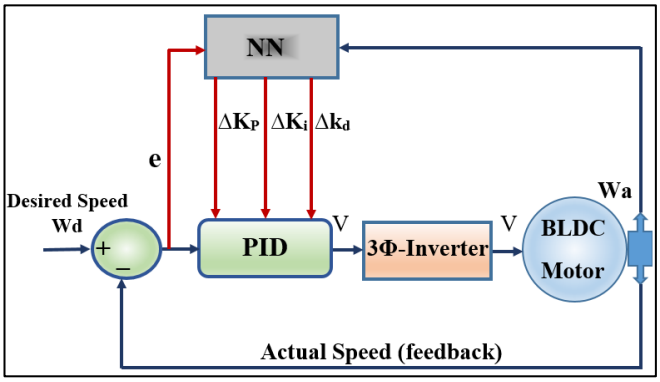

Fig. 16 Block schematic of the neural network-powered brushless DC motor.

Due to its late convergence rate and easiness of local minimum fallout, the traditional PID control approach can be less effective at times. Therefore, a created BP method was employed in this study. The goal of the current study was to successfully control the BLDC motor's rotor position utilizing a neural PID controller. The algorithm's training process convergence speed is excellent. Additionally, the trained BP neural network is highly adaptive and capable of self-learning [42]. Figure 17 provides a detailed illustration of the Neural-PID controller for a BLDC motor drive. One control block, rotor position control-Xoff (voltage control), is included with this particular controller.

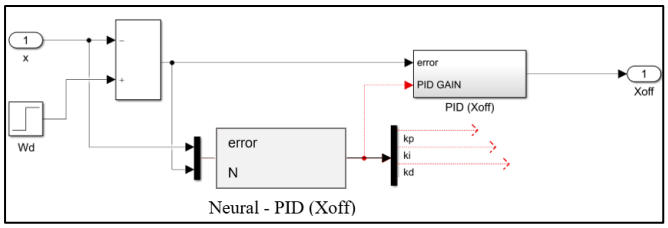

Fig. 17 Neural-PID Xoff controller.

In the PID neuron controller shown in Fig. 18, the rotor's position is controlled by the suggested controller, to obtain the traditional controller's settings, it is necessary to engage in a comprehensive analytical process, and adjust the output of the inverter (the output voltage that feeds the brushless motor), to ascertain the traditional controller's parameters and the inverter's output voltages, online, to determine the appropriate values for the stable operation of the brushless motor to achieve the actual speed at the output of the brushless motor, which corresponds to the required speed under varying loads and during any operating time and load.

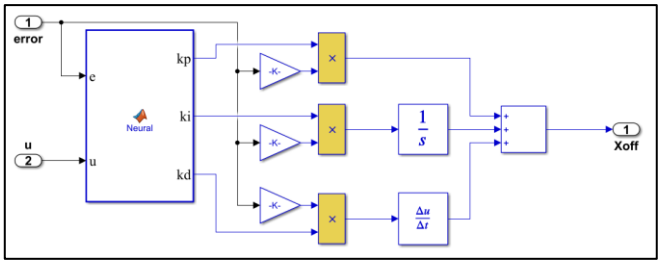

Fig. 18 Implemented Simulink model Neural-PID Xoff controller.

The controller's neural network structure is composed of two input neurons, namely error (e) and speed (N), The changes in the PID controller's parameter gains, together with five hidden neurons and three output neurons, are shown in Fig. 19.

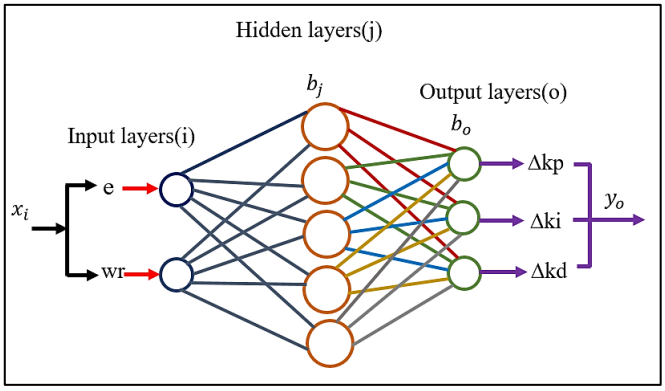

Fig. 19 the structure of NN.

The said controller has the following inputs and outputs:

$$\text{Xi} = \begin{bmatrix} e \\ N \end{bmatrix} \quad \text{and} \quad \text{y}_o = \begin{bmatrix} \Delta kp \\ \Delta ki \\ \Delta kd \end{bmatrix} \tag{11}$$

Where, the input vector of the neural network controller is represented by xi.

The output vector a neural network controller is represented by yo, which serves as a crucial component in the overall functioning of the system.

The mathematical formulation delineating the neural network can be computed by utilizing the subsequent equations [43], as per scholarly conventions.

$$\text{S}_j^K = \sum_{i=1}^{n} W_{ji}^K . Xi^K + b_j^K \tag{12}$$

$$y_j^K = \frac{1}{1+e^{-s_j^K}} \tag{13}$$

$$S_o^K = \sum_{j=1}^{K} W_{oJ}^K . y_j^K + b_o^K \tag{14}$$

$$y_o^K = \frac{1}{1+e^{-s_o^K}} \tag{15}$$

Where,

The hidden layers' output is shown as y_j^K.

The outputs of NN are y_o^K

W_{ji} is the weight of the input neurons to the hidden neurons.

W_{oj} is the ratio of the hidden neurons' weight to the output.

b_j^K is the concealed layers' bias.

b_o^K is the output layers' bias.

K is the present training set and K = 1: S

S is the whole count of training sets.

The Back-Propagation Algorithm, also known as BPA, is a well-known supervised learning technique used to train Artificial Neural Networks (ANNs). This approach is among the most prevalent forms of training methods utilized. BPA utilizes a gradient-descent optimization methodology, which is also known, when applied to feedforward networks, as the delta rule. A Multi-Layer Perceptron (MLP) is a feedforward network that has been trained using the delta rule [43].

The weights in this study are changed in the following ways using the delta rules equations of the BP algorithm:

$$\partial = y_o^K . (1 - y_o^K) . (d^K - y_o^K) \tag{16}$$

$$\partial_h = y_j^K * \left(1 - y_j^K\right) * W_{oj}^K * \partial \tag{17}$$

$$W_{oj}^{K+1} = W_{oj}^K + \partial * \eta * y_j^K \tag{18}$$

$$b_o^{K+1} = b_o^K + \partial * \eta \tag{19}$$

$$W_{ji}^{K+1} = W_{ji}^K + \partial_h * \eta * X_i^K \tag{20}$$

$$b_j^{K+1} = b_j^K + \partial_h * \eta \tag{21}$$

Where,

η: the learning rate, set 0.5, is.

∂: is the output neurons' delta rule.

The hidden neurons' delta rule is represented by ∂_h.

d^K: is the output result of NN.

The output is compared to the desired or goal output, and the following equation is used to determine the mean squared error at iteration k (ek):

$$e^K = 0.5 * (d_o^K - y_0^k)^2 \tag{22}$$

Training is repeated for all (k) patterns, where k is the current set or pattern. Then, the following equation is used to calculate the cumulative mean square error (Ce):

$$Ce = \sum_{K=1}^{S} e^K \tag{23}$$

The iterative process of training a neural network necessitates the repetition of the learning process for numerous cycles until the cumulative error reaches a sufficiently diminutive value. It is at this juncture that the training is deemed accomplished, and the altered weights are subsequently transferred to the BLDC motor neural network. This process involves the continuous refinement of the network's parameters, such as the weights and biases, by iteratively feeding the input data through the network and comparing the predicted outputs with the actual outputs. The aim is to minimize the error between the predicted and actual outputs, which is typically measured using a suitable loss function. Once the cumulative error reaches an acceptably low level, the training is considered complete, indicating that the neural network has learned the underlying patterns and relationships within the training data. The updated weights, which encapsulate the knowledge gained during the training process, are then applied to the BLDC motor neural network, enabling it to make accurate predictions or classifications based on new, unseen data.

The algorithm architecture of the BPA learning program is depicted in Fig. 20 through the use of a flow chart. In this flow chart, the input data (xi) is presented as a vector with a number of rows equal to (S) and a number of columns equal to the number of input neurons. Conversely, the desired output data (d) is represented as a column vector with S rows.

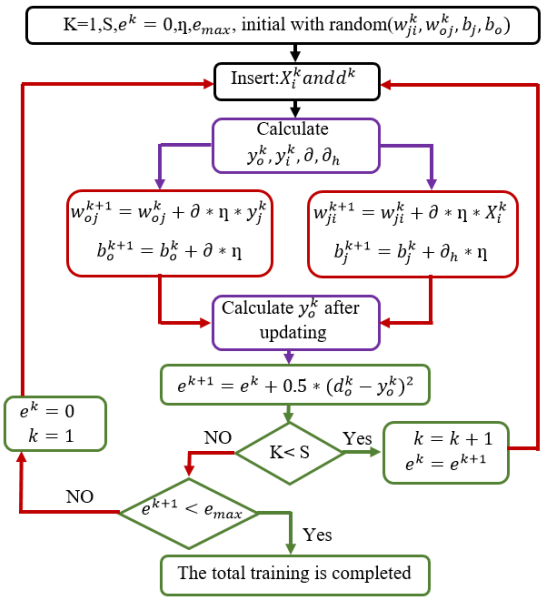

Fig. 20 Flow chart of the backpropagation training, adaptive [41].

It is worth noting that this particular representation plays a crucial role in facilitating the understanding and implementation of the BPA learning program. By visualizing the input data and desired output data in this manner, individuals can more effectively grasp the concepts and mechanics underlying the BPA learning program. Furthermore, this flow chart serves as a valuable reference tool during the implementation phase, aiding programmers in accurately translating the algorithm into code. Overall, the inclusion of this flow chart enhances the accessibility and usability of the BPA learning program, making it easier for individuals to comprehend and apply its principles. Table 2 and 3 show the advantages and disadvantages of the methods are used.

Table 2. the advantages of the methods are used.

No.	Advantages		
	PID	**GWO**	**ANN**
1	Simple and widely used in various applications.	Efficient for optimization problems and parameter tuning.	Can adapt to nonlinear and complex relationships in the motor system.
2	Quick response to changes in the system	Simple implementation and fewer parameters to adjust.	Suitable for online learning, it can improve performance over time.
3	A well-established and understood control method.	Can handle non-convex and multimodal optimization well.	Robust to noise and uncertainties in the system.

Table 3. the disadvantages of the methods are used.

No.	Disadvantages		
	PID	**GWO**	**ANN**
1	Limited effectiveness in handling complex and nonlinear systems.	May require fine-tuning of parameters for specific applications.	It requires a large amount of training data for accurate modeling.
2	Tuning PID parameters may require expertise and time.	In order to influence convergence speed, it is necessary to take into account the characteristics of the problem.	Complex structures may lead to increased computational requirements.
3	May exhibit steady-state error in certain situations.	Sensitivity to initial conditions.	Lack of transparency in decision-making.

To control the speed of BLDC motors, the choice between these methods depends on the specific application requirements. It depends on the available data and the desired trade-off between simplicity and adaptability. Combining these techniques or hybrid approaches may also improve performance. The most appropriate method for controlling the speed of a BLDC motor depends on a variety of factors.

1. Artificial neural networks (ANN) can provide an enhanced level of adaptability and performance for a system if its behavior is complex and non-linear and sufficient training data is available.
2. Gray Wolf Optimization (GWO) is an excellent choice if you are interested in optimizing and tuning parameters as well as reducing the amount of implementation work.
3. PID (Proportional Integral Derivative) controls can be an ideal solution if you need a simple and well-established control method that responds quickly to changes in the desired application.

6. Conclusion

Ultimately, the best way to achieve the desired performance requirements will depend on the characteristics of your system, the availability of data, and the specific performance requirements you are trying to achieve. For optimal performance, combining the strengths of different methods can also be considered as a hybrid approach, maximizing the strengths of each method.

It has been concluded that the artificial neural network (ANN) is one of the most promising methods for controlling the speed of BLDC motors. Artificial neural networks provide a powerful solution for neural systems within the motor system due to their ability to adapt to complex, nonlinear relationships within the system, as well as their ability to learn from data as they grow.

Although artificial neural networks require large training data to perform well, the associated computational load makes them a compelling choice for applications that require high adaptability and accuracy in motor control, despite the need for large training data.

References

[1] M. Niaz Azari, M. Samami, and S. Abedi Pahnekollaei, "Optimal design of a brushless dc motor, by cuckoo optimization algorithm (research note)," International Journal of Engineering, vol. 30, no. 5, pp. 668-677, 2017. https://doi.org/10.5829/idosi.ije.2017.30.05b.06

[2] S. R. Alwash, M. S. Al-Din, A. M. Eial-Awad, and J. Tafila, "Rotor Position Detection and Control for Spindle Brushless DC Motors Using Dummy Windings," 2011. https://doi.org/10.2316/P.2011.718-007

[3] S. Usha, P. M. Dubey, R. Ramya, and M. Suganyadevi, "Performance enhancement of BLDC motor using PID controller," International Journal of Power Electronics and Drive Systems, vol. 12, no. 3, p. 1335, 2021. https://doi.org/10.11591/ijpeds.v12.i3.pp1335-1344

[4] A. A. Obed and A. K. Kadhim, "Speed and current limiting control strategies for BLDC motor drive system: A comparative study," International Journal of Advanced Engineering Research and Science, vol. 5, no. 2, pp. 119-130, 2018. https://dx.doi.org/10.22161/ijaers.5.2.16

[5] H. Hu, T. Wang, S. Zhao, and C. Wang, "Speed control of brushless direct current motor using a genetic algorithm–optimized fuzzy proportional integral differential controller," Advances in Mechanical Engineering, vol. 11, no. 11, p. 1687814019890199, 2019. https://doi.org/10.1177/1687814019890199

[6] A. A. Obed, A. L. Saleh, and A. K. Kadhim, "Speed performance evaluation of BLDC motor based on dynamic wavelet neural network and PSO algorithm," International Journal of Power Electronics and Drive System (IJPEDS), vol. 10, no. 4, pp. 1742-1750, 2019. https://doi.org/10.11591/ijpeds.v10.i4.1742-1750

[7] M. Boonpramuk, S. Tunyasirut, and D. Puangdownreong, "Artificial intelligence-based optimal PID controller design for BLDC motor with phase advance," Indonesian Journal of Electrical Engineering and Informatics (IJEEI), vol. 7, no. 4, pp. 720-733, 2019.

https://doi.org/10.11591/ijeei.v7i4.1372
[8] A. L. Saleh, "Speed Control of Brushless DC Motor Based on PID and Wavelet Neural Networks," University of Basrah, 2014.
[9] H. Abdelfattah, M. I. Mosaad, and N. F. Ibrahim, "Adaptive neuro fuzzy technique for speed control of six-step brushless DC motor," Indonesian Journal of Electrical Engineering and Informatics (IJEEI), vol. 9, no. 2, pp. 302-312, 2021. https://doi.org/10.46300/91010.2021.15.10
[10] M. Yaz and E. Cetin, "Brushless Direct Current Motor Design and Analysis," COJ Electronics & Communications, vol. 2, no. 2, 2021. https://doi.org/10.31031/COJEC.2021.02.000534
[11] D. Mohanraj et al., "A review of BLDC Motor: State of Art, advanced control techniques, and applications," IEEE Access, vol. 10, pp. 54833-54869, 2022. https://doi.org/10.1109/ACCESS.2022.3175011
[12] M. Z. Haider, "Position Control of Permanent Magnet Brushless DC Motor using PID Controller," A Thesis, June -2011. http://hdl.handle.net/10266/1662
[13] M. Kumari, "Modelling, Simulation and Hardware Implementation of Speed Control of Brushless DC Motor," Master's Degree thesis, July, 2019.
[14] F. Nudo, "Numerical modeling of servomechanisms: comparison between different development environments," Master's Degree thesis, Politecnico di Torino, 2020.
[15] M. M. Ezzaldean, "Design of speed-controller for brushless dc-motor based on grey predictor-pid controller," Engineering and Technology Journal, vol. 36, no. 8A, pp. 900-905, 2018. https://doi.org/10.30684/etj.36.8A.9
[16] S. Rambabu, "Modeling and control of a brushless DC motor," Master of Thesis in Power Control and Drives Technology, National Institute of Technology Rourkela, 2007.
[17] M. Tawadros, "Sensorless Control of Brushless DC Motors," Ph.D. thesis, University of Western Sydney, December 2012.
[18] K. Sushita, and N. Shanmugasundaram, "Performance of BLDC motor with PI, PID and Fuzzy controller and its comparative analysis," European Journal of Molecular and Clinical Medicine, vol. 7, no. 8, pp. 2520–2524, 2020.
[19] M. Mahmud, S. Motakabber, A. Z. Alam, and A. N. Nordin, "Control BLDC motor speed using PID controller," International Journal of Advanced Computer Science and Applications, vol. 11, no. 3, 2020. https://doi.org/10.14569/IJACSA.2020.0110359
[20] A. Tashakori Abkenar, "BLDC motor drive controller for electric vehicles," Ph.D. thesis, Faculty of Science, Engineering and Technology, Swinburne University of Technology, 2014.
[21] J. C. Gamazo-Real, E. Vázquez-Sánchez, and J. Gómez-Gil, "Position and speed control of brushless DC motors using sensorless techniques and application trends," sensors, vol. 10, no. 7, pp. 6901-6947, 2010. https://doi.org/10.3390/s100706901
[22] A. p. S. Priya, "Speed Control of Brushless Dc Motor Using Fuzzy Logic Controller," IOSR Journal of Electrical and Electronics Engineering (IOSR-JEEE), vol. 10, no. 6 Ver. I, pp. PP 65-73, (Nov – Dec. 2015. https://doi.org/10.9790/1676-10616573
[23] M. R. Dodda Dinesh Kumar, Bonu Yogesh, Gandi Likhitha, "Control Techniques for BLDC Motor: A Review," International Journal of Research Publication and Reviews, vol. 3, no 11, pp. 294-302, 2022.
[24] B. Stefan, "BLDC motor modeling and control-A MATLAB/SIMULINK implementation," M. Sc. Thesis, Electrical Power Engineering, Chalmers University of Technology, Gothenburg, Sweden, 2005.
[25] A. J. V. R. Roy, and S. Thirunavukkarasu, "Optimized Speed Control for BLDC Motor," International Journal of Innovative Research in Science, vol. 3, Issue 1, pp. 1019-1030, 2014.
[26] H. N. Phyu, "Numerical analysis of a brushless permanent magnet DC motor using coupled systems," Ph.D. thesis, Department of Electrical & Computer Engineering, National University of Singapore, 2005.
[27] A. S. R. Murali Dasari, M Vijaya Kumar, "Adaptive Speed Control Algorithm for BLDC Motor with Variable Input Source using PSO Algorithm," International Journal of Innovative Technology and Exploring Engineering, vol. 9, Issue 2, pp. 994-1002, December 2019. https://doi.org/10.35940/ijitee.K1345.129219
[28] A. K. Hassan, M. S. Saraya, M. S. Elksasy, and F. F. Areed, “Brushless DC Motor Speed Control using PID Controller, Fuzzy Controller, and Neuro Fuzzy Controller,” International Journal of Computer Applications, vol. 180, no. 30, pp. 47–52, Apr. 2018. https://doi.org/10.5120/ijca2018916783
[29] D. K. Shary, H. J. Nekad, and M. A. Alawan, "Speed control of brushless DC motors using (conventional, heuristic, and intelligent) methods-based PID controllers," Indonesian Journal of Electrical Engineering and Computer Science, vol. 30, no. 3, pp. 1359-1368, 2023. https://doi.org/10.11591/ijeecs.v30.i3.pp1359-1368
[30] S. Mirjalili, S. M. Mirjalili, and A. Lewis, "Grey wolf optimizer," Advances in engineering software, vol. 69, pp. 46-61, 2014. http://dx.doi.org/10.1016/j.advengsoft.2013.12.007
[31] S. M. Almufti, H. B. Ahmad, R. B. Marqas, and R. R. Asaad, "Grey wolf optimizer: Overview, modifications and applications," International Research Journal of Science, Technology, Education, and Management, vol. 1, no. 1, pp. 44-56, 2021. https://doi.org/10.5281/zenodo.5195644
[32] A. K. Tripathi, K. Sharma, and M. Bala, "A novel clustering method using enhanced grey wolf optimizer and mapreduce," Big data research, vol. 14, pp. 93-100, 2018. https://doi.org/10.1016/j.bdr.2018.05.002
[33] B. Yang, X. Zhang, T. Yu, H. Shu, and Z. Fang, "Grouped grey wolf optimizer for maximum power point tracking of doubly-fed induction generator based wind turbine," Energy conversion and management, vol. 133, pp. 427-443, 2017. http://dx.doi.org/10.1016/j.enconman.2016.10.062
[34] M. A. ŞEN and M. Kalyoncu, "Optimal tuning of PID controller using grey wolf optimizer algorithm for quadruped robot," Balkan Journal of Electrical and Computer Engineering, vol. 6, no. 1, pp. 29-35, 2018. https://doi.org/10.17694/bajece.401992
[35] P. Dutta and S. K. Nayak, "Grey wolf optimizer based PID controller for speed control of BLDC motor," Journal of Electrical Engineering & Technology, vol. 16, pp. 955-961, 2021. https://doi.org/10.1007/s42835-021-00660-5

[36] M. H. Qais, H. M. Hasanien, and S. Alghuwainem, "A grey wolf optimizer for optimum parameters of multiple PI controllers of a grid-connected PMSG driven by variable speed wind turbine," IEEE Access, vol. 6, pp. 44120-44128, 2018. https://doi.org/10.1109/ACCESS.2018.2864303

[37] E. Emary, H. M. Zawbaa, and A. E. Hassanien, "Binary grey wolf optimization approaches for feature selection," Neurocomputing, vol. 172, pp. 371-381, 2016. https://dx.doi.org/10.1016/j.neucom.2015.06.083

[38] G. M. Fadhil, "Optimization the Performance of an AC Motor using Artificial Intelligent Techniques," M.Sc. thesis, Electrical Engineering Techniques, Southern Technical University, July 2020.

[39] S. M. Y. Younus, U. Kutbay, J. Rahebi, and F. Hardalaç, "Hybrid Gray Wolf Optimization–Proportional Integral Based Speed Controllers for Brush-Less DC Motor," Energies, vol. 16, no. 4, 2023. https://doi.org/10.3390/en16041640

[40] N. S. Shelke, S. Kumar "Neural Network Based BLDC Motor Speed Control," International Journal of Electrical, Electronics and Data Communication, vol. 7, no. 10, Oct.-2019.

[41] A. F. Abdulhasan, "Modeling and Control of Direct Drive surface (Planar) Motor", M.Sc. thesis, Electrical Engineering Techniques, Southern Technical University, June 2021.

[42] K. Mahmud, "Neural network based PID control analysis," 2013 IEEE Global High Tech Congress on Electronics, pp. 141-145, 2013. https://doi.org/10.1109/ghtce.2013.6767259

[43] L. Agrawal, B. Chauhan, N. Saxena, and P. Joshi, "Speed control of BLDC motor with the neural controller," Indian Journal of Science and Technology, vol. 14, no. 4, pp. 373-81, 2021. https://doi.org/10.17485/IJST/v14i4.2164